Neutron study of the magnetic-moment distribution in Co-Mn alloys

J. W. Cable
Solid State Division, Oak Ridge National Laboratory, Oak Ridge, Tennessee 37830
(Received 28 October 1981)

Magnetization and polarized-neutron diffuse-scattering measurements were made on Co-Mn alloys to determine the effects of local environment on their magnetic-moment distributions. Results show that the average ferromagnetic moment of Mn is small ($\sim 0.3\mu_B$) and antiparallel to the Co moments, which are large but decrease rapidly with increasing Mn content. Local environment effects are mainly confined to the Co moments with no indication of spatially correlated Mn moment fluctuations. It is concluded that the small Mn moment, relative to that usually observed for Mn in fcc alloys, is not due to a static distribution of parallel and antiparallel Mn moments. A dynamic fluctuation, as suggested by Jo and Miwa, may account for this low Mn moment.

INTRODUCTION

Magnetization data[1-5] for Co-Mn alloys show that both the spontaneous magnetization and the Curie temperature decrease linearly with increasing Mn content and vanish near 30 at.% Mn. The moment decrease is large (approximately $-4.5\mu_B$/Mn) and this led to the suggestion[2] that the Mn moments align antiparallel to the host magnetization. This was confirmed by unpolarized-neutron, diffuse-scattering measurements[6] which yielded an average Mn moment of $(-1.0 \pm 0.7)\mu_B$ for a Co–5 at.% Mn alloy. A dependence of the Co moments on their local environments was also determined from these data. More recently Nakai *et al.*[7] have examined more concentrated Co-Mn alloys using both polarized- and unpolarized-neutron methods. They report substantial agreement with the earlier unpolarized-neutron data, but their polarized-neutron data give positive Mn moments of about $0.3\mu_B$. They attributed this difference between the polarized and unpolarized results to the presence of Mn moments aligned both parallel and antiparallel to the Co moments. The corresponding Mn moment fluctuations could contribute additional scattering in the unpolarized method and lead to the observed difference. This assumption of the coexistence of parallel and antiparallel Mn moments has also been used to explain recent hyperfine field[8] and high-field susceptibility[9] data for this system. Such a coexistence of Mn magnetic states apparently occurs in the Ni-Mn system for which neutron data[10] show pronounced Mn moment fluctuations due to local environment effects. This concept is also supported by Hartree-Fock–coherent-potential approximation (HF–CPA) calculations[11-13] which indicate that either parallel or antiparallel Mn states may be stabilized under various local environment conditions. However, if a static distribution of these parallel and antiparallel states occurs in the Co-Mn system and if the moment direction depends on local environment, then the spatial correlations of these Mn moment fluctuations should be observed in the polarized-neutron cross section. Since no such correlation was observed,[7] and because of the uncertainty in the magnitude of the Mn moment, we have remeasured the polarized-neutron diffuse scattering from these alloys.

EXPERIMENTAL

Co-Mn alloys containing 5, 10, 15, 20, and 25 at.% Mn were prepared by arc melting and drop casting. These were machined into flat-plate neutron samples and rod-shaped magnetization samples which were homogenized for three days at 1270 K in a vacuum before quenching into water. Final concentrations were taken by attributing all weight losses to the Mn; these losses amounted to only 1–3% of the original Mn content. Neutron-diffraction patterns showed both hcp and fcc lines for all samples. The phase composition was estimated by comparison of the (101) hcp and (200) fcc intensities; this varied only from 40 to 50% fcc over the entire composition range. This phase mixture is not considered significant for this moment distribution study because identical magnetic diffuse cross sections have previously been observed[6] for Co-Mn samples of widely different phase composition.

The magnetization measurements were made by the extraction method at 4.2 K on 3-mm-diam rod samples in magnetic fields up to 3.2 T. Absolute values were obtained by calibration with a Ni sample for which a magnetization of $0.616\mu_B$/atom was assumed. The magnetizations are essentially saturated above 1.0 T so the spontaneous magnetizations are

readily obtained by extrapolation. The observed values (1.50, 1.33, 1.15, 0.85, and $0.55\mu_B$/atom for the 5, 10, 15, 20, and 25 at.% Mn alloys) lie in between those reported[1,2] for the fcc and hcp alloys as should be expected for these mixed phase samples.

The neutron measurements were made on 3-mm-thick flat-plate samples at 4.2 K in an applied field of 4 T. Diffuse intensity data were collected in the K range from 0.3 to 2.5 Å^{-1} for incident 1.067-Å neutrons polarized parallel and antiparallel to the sample magnetization. The intensities were corrected for instrumental polarizing and flipping efficiencies and for sample depolarization and converted to absolute cross sections by calibration with vanadium.

The disorder cross section from these alloys is given by[14]

$$\frac{d\sigma^{\pm}}{d\Omega}(K) = c(1-c)[\Delta b^2 S(K) \pm 0.54\Delta b \mathfrak{M}(K) + (0.27)^2 T(K)] \ , \quad (1)$$

where c is the Mn concentration, Δb is the nuclear amplitude difference, $b_{\mathrm{Mn}} - b_{\mathrm{Co}}$, and the $\pm$ sign denotes the neutron polarization relative to the sample magnetization. The scattering functions $S(K)$, $\mathfrak{M}(K)$, and $T(K)$ are Fourier transforms of the atom-atom, atom-moment, and moment-moment spatial correlations. The $\mathfrak{M}(K)$ and $T(K)$ correlations include atom-atom correlations and, in the absence of nonlinear response, these can be taken into account by use of the expressions $\mathfrak{M}(K) = S(K)M(K)$ and $T(K) = S(K)M(K)^2$, where $M(K)$ is the atom-moment correlation in the absence of atomic short-range order (SRO). These Co-Mn alloys exhibit only slight departures from randomness as is illustrated in Fig. 1 which shows the sum of the spin-up and spin-down cross sections for the 20% at. Mn alloy. This sum cross section contains the $S(K)$ and $T(K)$ disorder terms of Eq. (1) along with the spin-incoherent (0.68 b) and multiple Bragg (0.05 b) cross sections. The open data points in the figure represent the observed cross sections while the solid points have been corrected for the $T(K)$ term by assuming $T(K) = M(K)^2$ with $M(K)$ taken from the difference between the spin-up and spin-down cross sections. The solid line is the sum of the incoherent and multiple Bragg scattering which is assumed to be independent of K. The nuclear disorder scattering is then the difference between the solid points and the solid line. This scattering shows little K dependence except for a slight peaking near $K = 1.75$ Å^{-1} which suggests a small amount of SRO. In terms of $S(K)$, this peak departs from unity by only 10–15% which corresponds to $\alpha(R_1) \simeq -0.05$ if all SRO effects are attributed to nearest neighbors. Since this effect is barely outside of experimental error, even at this high-concentration level, we neglect it and assume random alloys $[S(K) = 1]$ for the analyses of the difference cross sections.

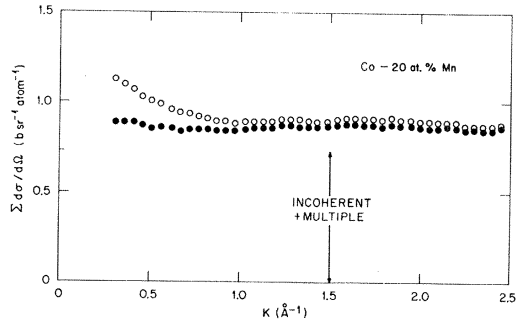

FIG. 1. The sum of the spin-up and spin-down cross sections for a Co–20 at.% Mn alloy. The open data points are observed while the solid points have been corrected for the $T(K)$ term in Eq. 1. The solid line is the level of incoherent and multiple Bragg scattering.

The difference between the spin-up and spin-down cross sections contains only the $\mathfrak{M}(K)$ term in Eq. (1) plus the difference in multiple Bragg scattering for spin-up and spin-down neutrons. The latter was calculated using standard methods and the observed spin-dependent transmissions. Although the correction procedure is only approximate, it was cross checked by comparison of the calculated (9 mb) and observed (6 ± 2 mb) effect for a pure Co sample. The corrections are similar in magnitude for the alloys and range from 5 to 15% of the observed difference cross sections. The $M(K)$ functions obtained from these corrected difference cross sections using $b_{\mathrm{Co}} = 0.250$ and $b_{\mathrm{Mn}} = 0.373 \times 10^{-12}$ cm are shown in Fig. 2. All of these are similar in shape with forward direction peaks that decay into flat regions at large K. The peaks correspond to moment correlations over a few neighbor distances and the flat regions have magnitudes that are approximately $\Delta\mu = \bar{\mu}_{\mathrm{Mn}} - \bar{\mu}_{\mathrm{Co}}$.

In the linear response model of Marshall,[15] $M(K)$ is given by

$$M(K) = \bar{\mu}_{\mathrm{Mn}} f_{\mathrm{Mn}}(K) - \bar{\mu}_{\mathrm{Co}} f_{\mathrm{Co}}(K) + (1-c)G(K) f_{\mathrm{Co}}(K) + cH(K) f_{\mathrm{Mn}}(K) \ , \quad (2)$$

where $\bar{\mu}_{\mathrm{Mn}}$ and $\bar{\mu}_{\mathrm{Co}}$ are the average Mn and Co moments, $G(K)$ and $H(K)$ are the K dependent moment disturbances at Co and Mn sites, and $f(K)$ is the magnetic form factor of the subscripted atom. Since $G(K)$ and $H(K)$ have the same K dependences and therefore cannot be separately determined, we combine the last two terms of Eq. (2) into a $\phi(K)$ function and fit the data to the expression

$$\frac{M(K)}{f_{\mathrm{Co}}(K)} = \Delta\mu + \sum_{R \neq 0} z(R_i)\phi(R_i)\frac{\sin KR_i}{KR_i} \ . \quad (3)$$

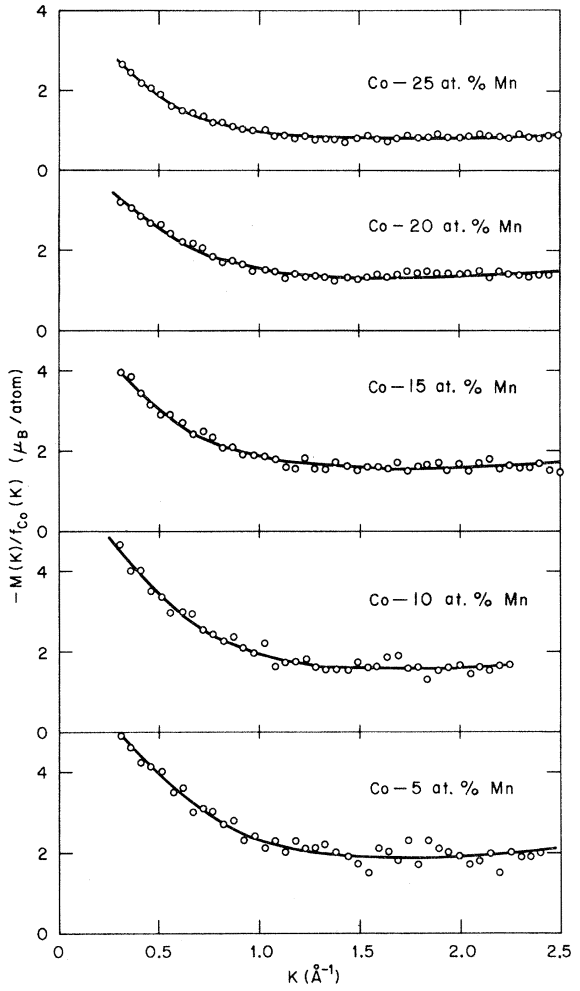

FIG. 2. Moment disturbance functions for Co-Mn alloys. Solid curves are fitted to Eq. (3) with the parameters of Table I.

Here, $\phi(R_i)$ is the concentration-weighted sum of the moment disturbance at Co and Mn sites caused by a Mn site occupation fluctuation at distance R_i and $Z(R_i)$ is the number of atoms at that distance. We approximate the form factor by $f_{Co}(K) = \exp(-0.049K^2)$ and use the fcc lattice to define $Z(R_i)$. We further assume an exponential decay for $\phi(R_i)$ of the form

$$\phi(R_i) = \frac{R_1}{R_i}\phi(R_1)\exp[-\kappa(R_i - R_1)] \ , \qquad (4)$$

and fit with the parameters $\Delta\mu$, $\phi(R_1)$, and κ, the inverse correlation length. The best fits are represented by the solid curves in Fig. 2 with the parameters in Table I. Also given are $M(0)$ values which are the $M(K)$ evaluated at $K = 0$ using the fitted parameters. If all moment disturbances are due to local environment effects then $M(0)$ should equal $d\bar{\mu}/dc$. Although magnetization data[2] give a constant $d\bar{\mu}/dc$ of about $-4.5\mu_B$/Mn over this concentration region, our fitted $M(0)$ values tend to decrease with increasing Mn content. We do not attach much significance to this difference since the experimental uncertainty in both $M(0)$ and $d\bar{\mu}/dc$ is about 10%. Clearly, most of the magnetization decrease is associated with the local environment effects accessible to this neutron technique. This dependence on local environment allows an estimate of the individual Co and Mn contributions to $\phi(R_i)$ by comparison of the concentration dependence of the average moments with the relations $G(0) = d\bar{\mu}_{Co}/dc$ and $H(0) = d\bar{\mu}_{Mn}/dc$ given by Marshall.[15] Average Co and Mn moments are obtained by combining the $\Delta\mu$ parameters from Table I with the magnetizations extrapolated to the 4.0-T field condition of the neutron measurements. Results are given in Table II and Fig. 3 where the error limits given include the statistical and fitting errors along with the uncertainties in the instrumental and multiple Bragg scattering corrections. The results show a large, positive $\bar{\mu}_{Co}$ that decreases rapidly with concentration and a small, negative $\bar{\mu}_{Mn}$ with little concentration dependence. Since $d\bar{\mu}_{Mn}/dc$ is small and positive while $M(0)$ is negative, it is

TABLE I. Moment disturbance parameters for Co-Mn alloys.

c	$\Delta\mu$[a]	$\phi(R_1)$[a]	K(Å^{-1})	$M(0)$[a]
0.050	−2.16	−0.143	0.55	−6.0
0.097	−1.84	−0.127	0.51	−5.8
0.147	−1.77	−0.102	0.47	−5.2
0.198	−1.51	−0.082	0.47	−4.3
0.244	−0.91	−0.073	0.38	−4.1

[a] μ_B/atom.

TABLE II. Average moments for Co-Mn alloys.

c	$\bar{\mu}$[a]	$\bar{\mu}_{Co}$	$\bar{\mu}_{Mn}$
0.050	1.52	1.63	−0.53 ±0.12
0.097	1.36	1.54	−0.30 ±0.09
0.147	1.18	1.44	−0.33 ±0.09
0.198	0.88	1.18	−0.33 ±0.06
0.244	0.58	0.80 ±0.01	−0.11 ±0.04

[a] Magnetization at 4 T (extrapolated).

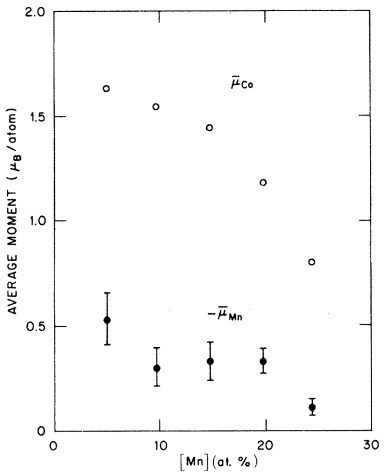

FIG. 3. Concentration dependence of the average ferromagnetic moments of Co and Mn in Co-Mn alloys. Note that the Mn moments are negative.

clear that $G(K)$ is the dominant K-dependent term in $M(K)$. Thus, the moment disturbance effects caused by a Mn site occupation fluctuation occur mostly at the Co sites. The parameters of Table I show that about one-third of the total moment disturbance, $M(0)$, comes from $\Delta\mu$, which is just the on-site effect of replacing a Co moment by a Mn moment. The rest of the disturbance derives from moment fluctuations on neighboring Co sites. $\phi(R_1)$ decreases fairly rapidly with Mn content but this is compensated by a simultaneous increase in the range of $\phi(R_l)$ so that $M(0)$ shows only the slight concentration dependence shown in Table I.

CONCLUSIONS

These results show that the average ferromagnetic moment of Mn in Co is small ($\sim 0.3\mu_B$) and antiparallel to the host magnetization. Local environment effects are observed but these consist mainly of moment fluctuations on Co sites surrounding a Mn site occupation fluctuation. Spatially correlated Mn moment fluctuations are not observed so that any static coexistence of parallel and antiparallel Mn moments requires a random distribution of such states. This seems unlikely in view of the strong spatial correlation of these states in Ni-Mn alloys.[10] A more likely explanation of this drastic reduction in $\bar{\mu}_{Mn}$ from the 3 to $4\mu_B$ usually observed for Mn in fcc systems is a dynamic fluctuation between parallel and antiparallel states as suggested by Jo and Miwa.[12] In their calculations they find small energy differences between the two states and suggest that dynamical fluctuations may be important even at low temperatures. In that event, the neutron results would yield a moment value in between the parallel and antiparallel moment values.

ACKNOWLEDGMENT

This research was sponsored by the Division of Materials Sciences, U.S. Department of Energy, under Contract No. W-7405-ENG-26 with the Union Carbide Corporation.

[1]C. Sadron, Ann. Phys. 17, 371 (1932).
[2]J. Crangle, Philos. Mag. 2, 659 (1957).
[3]J. S. Kouvel, J. Phys. Chem. Solids 16, 107 (1960).
[4]M. Matsui, T. Ido, K. Sato, and K. Adachi, J. Phys. Soc. Jpn. 28, 791 (1970).
[5]D. R. Rhiger, D. Muller, and P. A. Beck, J. Magn. Magn. Mater. 15–18, 165 (1980).
[6]J. W. Cable and T. J. Hicks, Phys. Rev. B 2, 176 (1970).
[7]Y. Nakai, K. Hozaki, and N. Kunitomi, J. Phys. Soc. Jpn. 45, 73 (1978).
[8]H. Yasuoka, H. Hoshinouchi, and Y. Nakamura, J. Phys. Soc. Jpn. 34, 1192 (1973).
[9]N. Kunitomi, Y. Nakai, T. Sakakibara, H. Mollymoto, and M. Date, J. Phys. Soc. Jpn. 48, 1777 (1980).
[10]J. W. Cable and H. R. Child, Phys. Rev. B 10, 4607 (1974).
[11]H. Hasegawa and J. Kanamori, J. Phys. Soc. Jpn. 33, 1599 (1972).
[12]T. Jo and H. Miwa, J. Phys. Soc. Jpn. 40, 706 (1976).
[13]T. Jo, J. Phys. Soc. Jpn. 40, 715 (1976).
[14]R. A. Medina and J. W. Cable, Phys. Rev. B 15, 1539 (1977).
[15]W. Marshall, J. Phys. C 1, 88 (1968).